Development of *N*-glycan Microarrays as Sensors for Glycan Binders

Abstract

There is a pressing need for rapid, cost-effective, and sensitive viral detection platforms; the recent COVID-19 outbreak highlighted the drawbacks of current detection platforms. Sialylated N-glycans have been found to play a role in the SARS-CoV-2[1] and Influenza A virus attachment to host cells. Our aim is to illustrate the potential of sialo-glycan-functionalized microarrays for sensitive lectin detection and discrimination and to create a viral sensor that can simultaneously detect multiple viruses.

N-glycan Structure and Polymerization

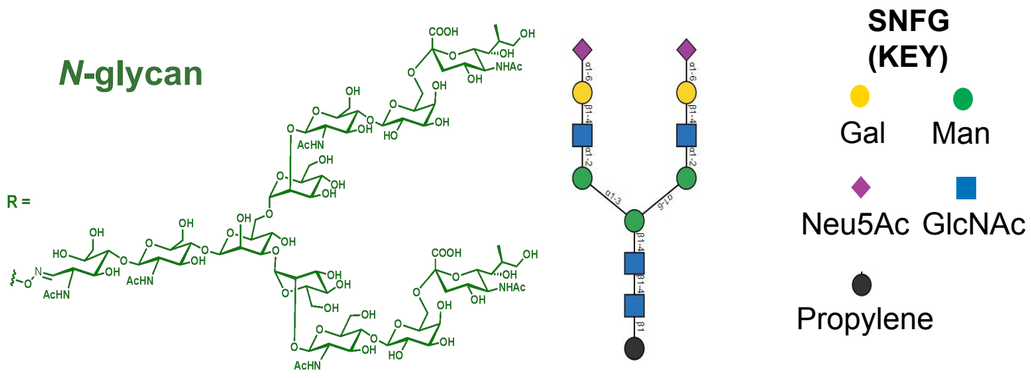

Neu5Aca1-6Galb1-4GlcNAca1-2Mana1-6(Neu5Aca1-6Galb1-4GlcNAc a1-2Mana1-3)Manb1-4GlcNAcb1-4GlcNAcb1-propylene

Figure 1: *N*-Glycan structure. From SI in Broad-spectrum synthetic carbohydrate receptors (SCRs) inhibit viral entry across multiple virus families, by Ezzatpour, S., et al., 2025, *Science Advances, 11*, (https://doi.org/10.1126/sciadv.ady3554).

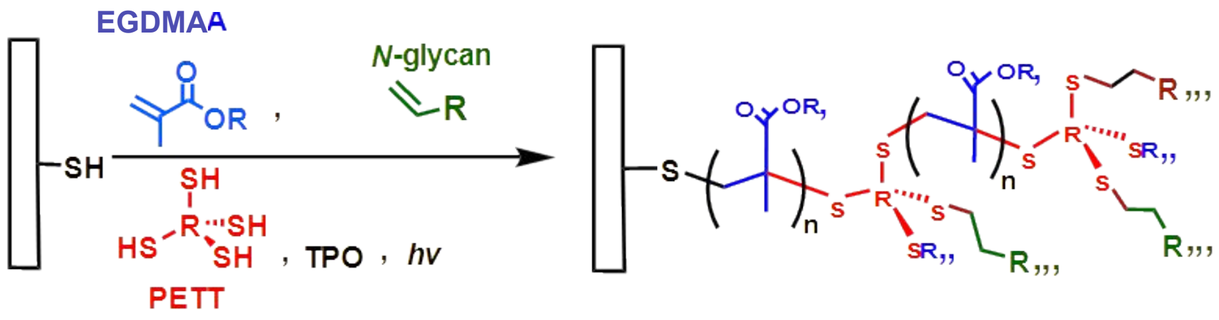

Scheme 1: Immobilization of *N*-Glycan using GTGFRP. From SI in Broad-spectrum synthetic carbohydrate receptors (SCRs) inhibit viral entry across multiple virus families, by Ezzatpour, S., et al., 2025, *Science Advances, 11*, (https://doi.org/10.1126/sciadv.ady3554).

Optimizing Printing of N-Glycan-functionalized Polymer Brush Microarrays

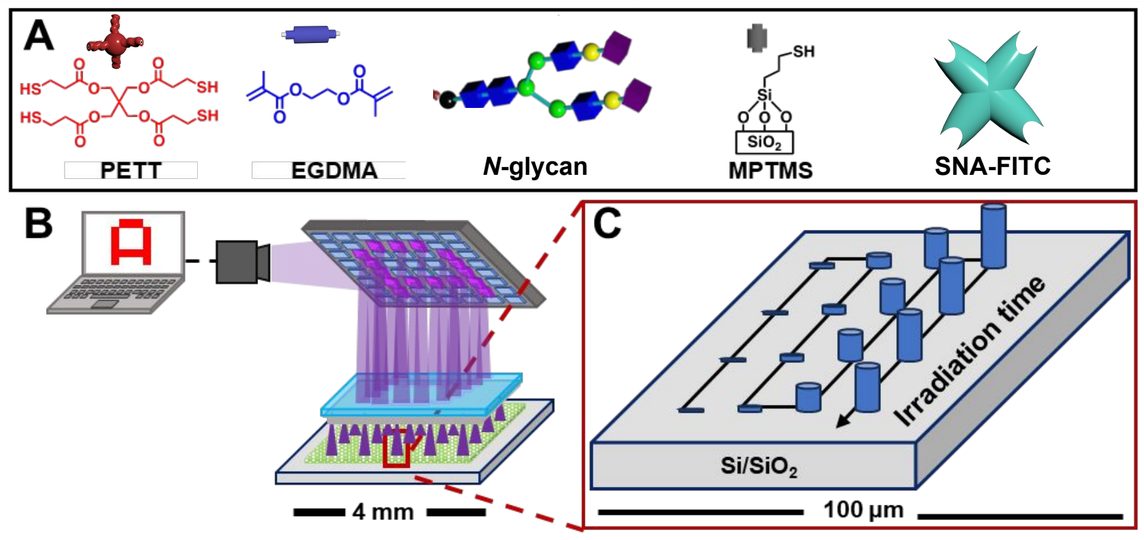

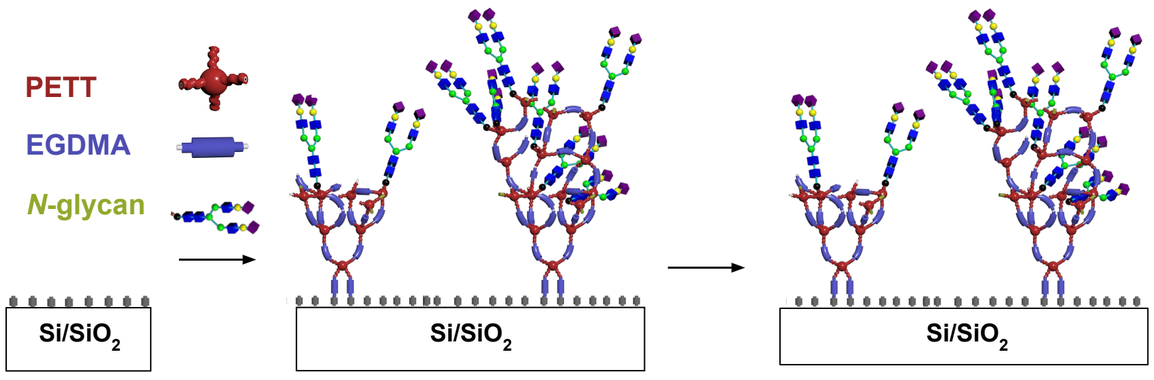

Figure 3: (A) Legend of elements involved in the printing of *N*-Glycan-functionalized polymer brushes. (B) The hypersurface photolithography (HP) printer used in microarray preparation combines a digital micromirror device, a fluid cell, and grafted-from surface chemistry to create patterns. (C) Microarrays of polymer brushes with varying heights at each feature are prepared by varying the irradiation time of each feature during printing. (D) Scheme of *N*-Glycan/EGDMA/PETT grafted on a surface. Adapted from Figure 2 A, B, C in *Monosaccharide binding to synthetic carbohydrate receptor microarrays*, by Shlain, M. A., Ndede, K. E., Thakur, K., Russo, A. J., Pasari, S., Nihal, I., Matos, K. L., Zholdassov, Y. S., Marianski, M., & Braunschweig, A. B., 2025, *The Journal of Physical Chemistry C, 129*(46), 20797–20808 (https://doi.org/10.1021/acs.jpcc.5c06186).

N-Glycan Print Validation and Optimization

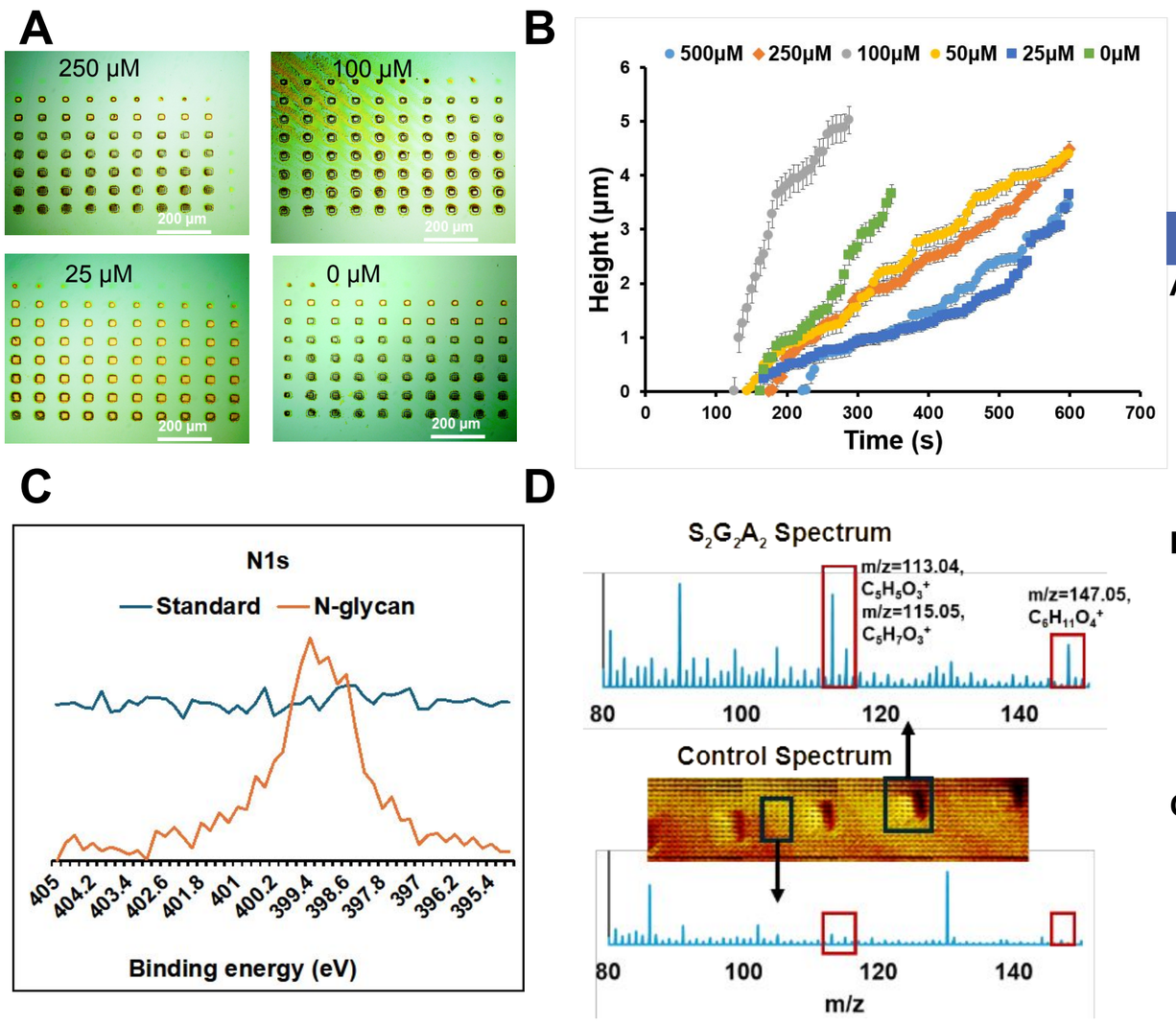

Figure 2: (A) Optical images of different concentration ***N*-glycan**-functionalized polymer brush microarrays. (B) Graph showing effect of varying ***N*-glycan** concentration on polymer brush height ([PETT] = 100 mM [EGDMA] =1300 mM; [TPO] = 1 mM; light intensity = 2.53 mW·mm^{-2} , [***N*-glycan**] = 500 µM, 250 µM, 100 µM, 50 µM, 25 µM, 0 µM). (C) XPS of polymer brush patterns containing ***N*-glycan**-functionalized brush polymers ([PETT] = 100 mM [EGDMA] =1300 mM; [TPO] = 1 mM; light intensity = 2.53 mW·mm^{-2} , [***N*-glycan**] = 500 µM) and ("standard") polymer brush features, which were printed without ***N*-glycan** ([PETT] = 100 mM [EGDMA] =1300 mM; [TPO] = 1 mM; light intensity = 2.53 mW·mm^{-2} , [***N*-glycan**] = 0 µM).(D) TOF-SIMS Analysis of N-glycan Functionalized Surface with the same print conditions as (C). Adapted from Figure 5 D, E in Broad-spectrum synthetic carbohydrate receptors (SCRs) inhibit viral entry across multiple virus families, by Ezzatpour, S., et al., 2025, *Science Advances, 11*, (https://doi.org/10.1126/sciadv.ady3554).

Selectivity of *N*-Glycan Microarrays Towards different Lectins

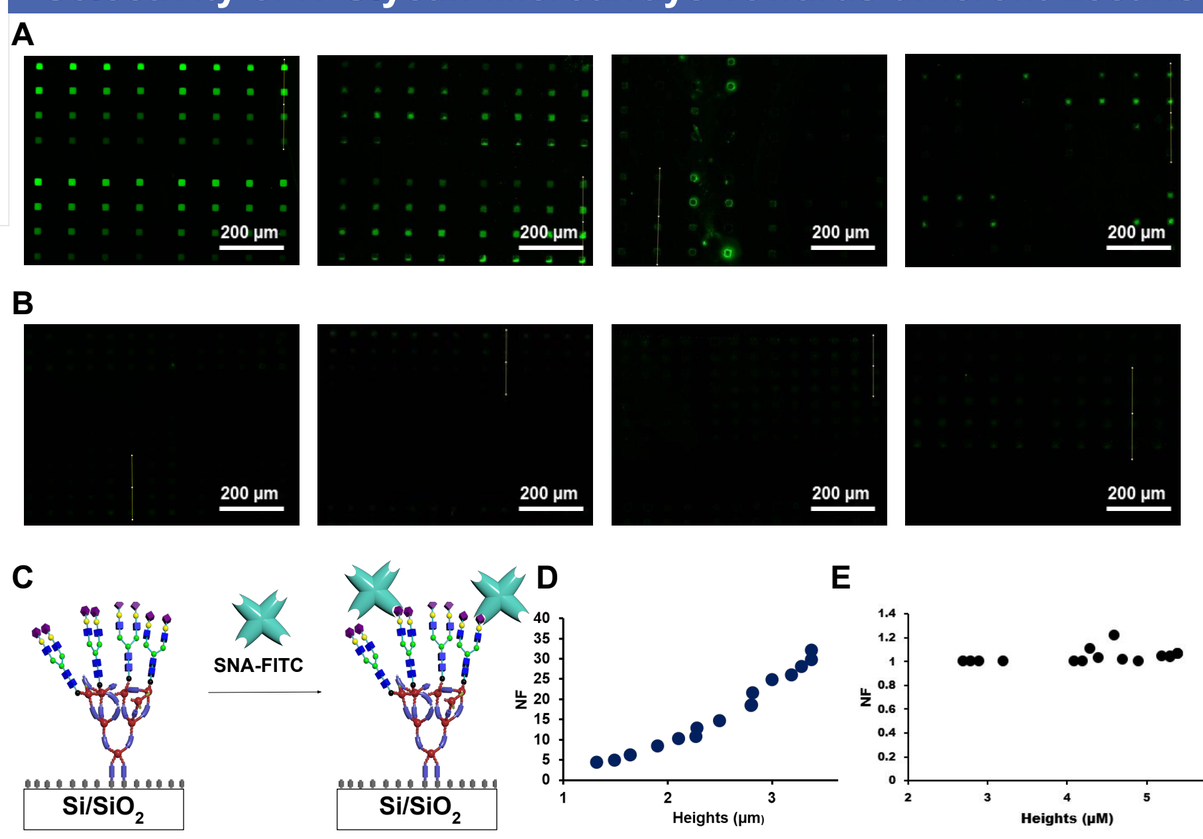

Figure 4: (A) Fluorescent micrograph showing concentration dependent binding between ***N*-glycan**-functionalized brush polymers [***N*-glycan**] = 25 µM, 50 µM, 100 µM, 250 µM respectively with **SNA-FITC** (2 mg/mL) in HEPES buffer. (B) Fluorescent micrograph showing concentration dependent binding between ***N*-glycan**-functionalized brush polymers [***N*-glycan**] = 25 µM, 50 µM, 100 µM, 250 µM respectively with **ECA-FITC** (2 mg/mL) in HEPES buffer. (C) Binding of ***N*-glycan**-functionalized brush polymers with SNA-FITC (D) Graph charting the NF (or *I*) compared to polymer brush height in ***N*-glycan**-functionalized microarrays prepared under the same conditions and [***N*-glycan**] = 25 µM incubated with **SNA-FITC**. (E) Graph charting the NF compared to polymer brush height in ***N*-glycan**-functionalized microarrays prepared under the same conditions incubated with **ECA-FITC**. Figure created by student researcher. Graphs created by student researcher using Excel in 2024.

Conclusion

- HP controls polymerization, with polymer brushes growing at around 200 seconds under 405 nm light at a light intensity of 2.53 mW/mm^2.
- Different concentrations of *N*-Glycan print differently, with the tallest brushes observed at 100µM.
- The microarrays successfully distinguished between lectins: Sambucus Nigra Lectin, fluorescein (SNA-FITC) and Erythrina Cristagalli Lectin, fluorescein (ECA-FITC).

Next Steps

- Incubation with multiple concentrations of lectins
  - SNA-FITC as positive control
  - ECA-FITC as negative control
- Creation of surface with multiple *N*-Glycans to simultaneously detect for multiple viruses
- Development of AI model to analyze fluorescence binding of each virus to create a "binding fingerprint"

Works Cited

1. Saso, Wakana, Masako Yamasaki, Shin-ichi Nakakita, Shuetsu Fukushi, Kana Tsuchimoto, Noriyuki Watanabe, Nongluk Sriwilaijaroen, et al. 2022. "Significant Role of Host Sialylated Glycans in the Infection and Spread of Severe Acute Respiratory Syndrome Coronavirus 2." PLOS Pathogens 18 (6): e1010590–90. https://doi.org/10.1371/journal.ppat.1010590.
2. McQuillan, Alyssa M., Lauren Byrd-Leotis, Jamie Heimburg-Molinaro, and Richard D. Cummings. 2019. "Natural and Synthetic Sialylated Glycan Microarrays and Their Applications." Frontiers in Molecular Biosciences 6 (September). https://doi.org/10.3389/fmolb.2019.00088.
3. Ji Young Hyun, Jaeyoung Pai, and Injae Shin. 2017. "The Glycan Microarray Story from Construction to Applications." Accounts of Chemical Research 50 (4): 1069–78. https://doi.org/10.1021/acs.accounts.7b00043.

Pasari, S.